Long Throw with Casting Probe System

Hitoshi Arisumi*, Masatsugu Otsuki**, Takeshi Hoshino**

*National Institute of Advanced Industrial Science and Technology (AIST), Japan
e-mail: h-arisumi@aist.go.jp

**Japan Aerospace Exploration Agency (JAXA), Japan
e-mail: {otsuki.masatsugu, hoshino.takeshi}@jaxa.jp

Abstract

In this paper, we firstly discuss how to put the probe vehicle on the bottom of the vertical hole discovered on the surface of the moon. We then propose a method of throwing the probe into the hole to speed up the transportation, reduce energy consumption, and avoid influence of geological factors. In order to achieve the two conflicting goals, i.e. high-precision throw and long throw, we elucidate suitable throwing mode and its control parameters for reduction of the error of the landing position of the probe. We finally develop the casting probe system for high speed rotation, and realize the long throw of high precision with it.

1 Introduction

The JAXA lunar orbiter spacecraft "SELENE (Kaguya)" discovered giant vertical holes on the surface of the moon as shown in Fig. 1. The holes are presumed to be skylights of subsurface caverns such as lava tubes or magma chambers as shown in Fig. 2. These holes and caverns are very significant for lunar sciences because of untouched original environment free from cosmic dust. In addition, they are promising candidates for lunar base with laboratory facilities because they are regarded as a natural shelter free from meteorite impacts, high-energy ultraviolet rays, radiation, or extreme diurnal temperature variations (more than 300K) [1, 2]. They thus could be high-priority targets of future lunar exploration. For these reasons, it is expected to develop techniques to approach this new world. We here discuss how to use the robot technology to put the probe on the bottom of the vertical hole from the lander.

The area around the vertical hole is considered to be fragile as the hole was formed by collapse of the roof of underlying caverns [2]. Furthermore, high precise landing techniques are still in a developmental stage. Therefore, the touchdown point of the lander should be a long way from the vertical hole. Mobile robots thus are needed to carry the probe from the lander to the hole after touchdown. Following well-known technologies, a rover robot may be a dominant way to approach the hole. However, it is still difficult for the rover to move through wasteland containing features such as rugged surface or regolith because the system down caused by tumble or being stuck may occur there. Even if possible, the rover also cannot easily get close to the hole due to the fragility around it.

To overcome the difficulties, we apply casting manipulator system [3] to the exploration of the holes and the caverns. The sequential motion phases are shown in Fig. 2; a) rotation of a boom of the casting probe system to store the kinetic energy, b) release of a capsule which contains a probe vehicle, c) flight of the capsule, d) inflation of balloon before landing to absorb the landing shock, e) the vehicle gets out of the capsule and starts to explore the caverns, f) the vehicle returns to the capsule and the whole system is pulled back to the origin by reeling up wire. A key feature of the casting probe system is the ability to move the capsule quickly independent of several kinds of landforms or geological conditions. Compared to the other robots, it can be thought that the casting probe system is excel at the viewpoint of working time, energy consumption, step number of motions, and fault tolerance.

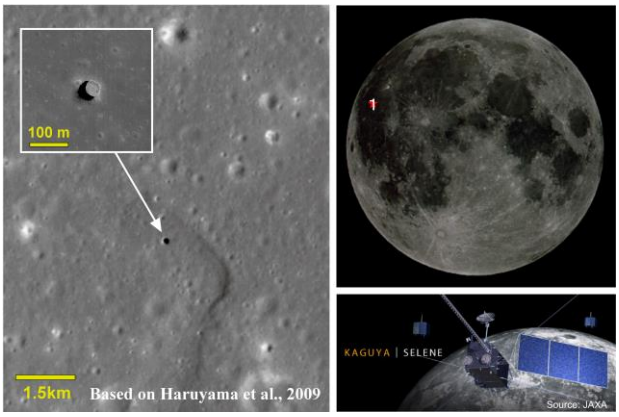

Figure 1: Lunar vertical hole (Marius Hills in Oceanus Procellarum)

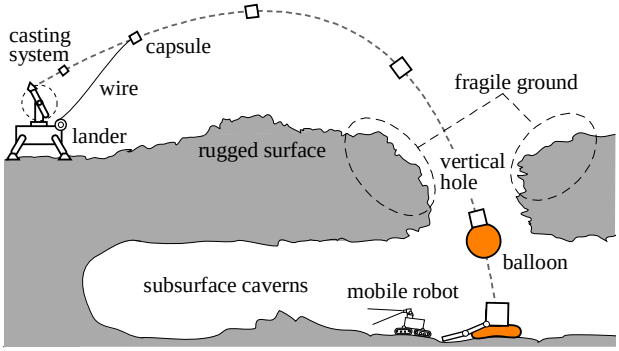

Figure 2: Throwing-down scenario

We mainly discuss two topics in this paper: how to decide the launch parameters to reduce a landing position error of the capsule, and how to realize a long throw with the hardware.

2 Throwing method

For the first topic, we focus on the timing error of releasing the capsule as main factor of generating the error of landing position. We thus analyze the landing position error with respect to the release angle varying the rotational speed.

2.1 Related works

In general, the thruster such as liquid/solid rocket is mainly used for a flight in the space. But the thruster may not be a suited travel device for continuous exploration on the moon because its propellant is consumed. For that reason, we do not use consumable energy sources such as propellant for launch of a capsule. Instead, we use electricity supplied by the solar power generation system for drive of the electric actuators.

In robotics filed, several kinds of mechanisms or control methods to launch an end-effector/object are studied, which are classified as a dexterous manipulation. In these studies, launches are divided broadly into two types, launch by translation and that by rotation. Kaneko et al. proposed "100G Capturing robot" which utilizes spring energy for launching a light arm/gripper at a high speed [4]. They realized launch of the gripper by its translational motion. The launch mechanism is simple thanks to use of the spring indeed, but characteristics of the elastic materials such as the spring typically change with frequency in use. In case of using the linier actuator for translational launch in place of the spring, very long track is needed to accelerate the end-effector to throw further. It causes the system enlarged. For this reason, we address rotational launch in this paper.

Tabata and Aiyama [5] proposed the tossing manipulation in which an object is thrown by swinging the arm with sliding the object on it. Throwing method itself is unique indeed, but uncertain factors such as friction makes tossing control even harder. In addition, continuous rotational motion of the arm may be needed to throw the object further, but it is difficult to realize it because the object is free on the arm.

2.2 Underarm throw vs sidearm throw

There are various sorts of throwing by rotation, but we here focus on two typical throwing methods, underarm throw and sidearm one. Figure 3(a) shows the underarm throw of capsule where a plane of the boom's rotation is vertical, while Fig. 3(b) shows the sidearm throw where a plane of its rotation is horizontal or diagonal. In order to compare their performances, we analyze accuracy of landing position of capsule thrown by each method. We assume that rotational velocity of the boom is constant and the actual release point P_r deviates from the desired release point P_d. For simplicity, tension of the wire is ignored.

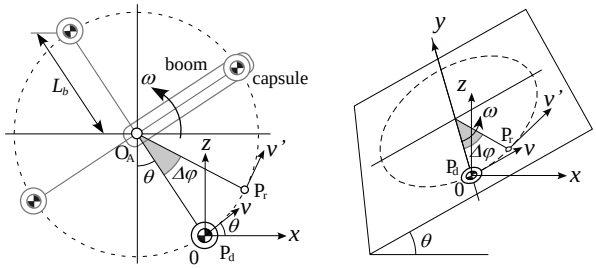

(a) Underarm throw (b) Sidearm throw

Figure 3: Two throwing modes by using rotation

As shown in Fig. 3, the origin of an xyz Cartesian coordinate system is set at P_d and directions of z-axis is set in the negative direction of gravity. x-axis is included in the rotation of the plane as shown in Fig. 3(a), while y-axis is set on horizontal plane and it passes through the center of rotation as shown in Fig. 3(b). For both throw, L_b, ω, and θ in Fig. 3 denote a length of the boom, rotational velocity of the boom, and the desired elevation angle of releasing the capsule, respectively. $\Delta\varphi$ is angular error of rotation, and v' is release speed of the capsule.

The release position vector ${}^i\boldsymbol{P}_r({}^ix_r, {}^iy_r, {}^iz_r)$ and release speed vector ${}^i\boldsymbol{v}'({}^iv_x, {}^iv_y, {}^iv_z)$ at P_r are given by the followings:

$$
\begin{aligned}
&{}^a\boldsymbol{P}_r(L_b(\sin(\theta+\Delta\varphi)-\sin\theta),\ 0,\ L_b(\cos\theta-\cos(\theta+\Delta\varphi))),\\
&{}^a\boldsymbol{v}'(v'\cos(\theta+\Delta\varphi),\ 0,\ v'\sin(\theta+\Delta\varphi)),
\end{aligned}
$$

$^{b}\boldsymbol{P}_{\mathrm{r}}\,(L_b \sin\Delta\varphi \cos\theta,\ L_b\,(1-\cos\Delta\varphi),\ L_b \sin\Delta\varphi \sin\theta)$,
$^{b}\boldsymbol{v}'(v'\cos\Delta\varphi \cos\theta,\ v'\sin\Delta\varphi,\ v'\cos\Delta\varphi \sin\theta)$,

where $v' = L_b\omega$, and superscripts i (= a, b) represent symbol concerning underarm throw and sidearm one, respectively. Using $^{i}\boldsymbol{P}_{\mathrm{r}}$ and $^{i}\boldsymbol{v}'$, landing position vector $^{i}\boldsymbol{P}_{\mathrm{f}}$ ($^{i}x_f$, $^{i}y_f$, $^{i}z_f$) is given by

$$^{i}x_f = {}^{i}v_x\, t_f + {}^{i}x_r\ , \quad (1)$$
$$^{i}y_f = {}^{i}v_y\, t_f + {}^{i}y_r\ , \quad (2)$$
$$^{i}z_f = -0.5g\, t_f^{2} + {}^{i}v_z\, t_f + {}^{i}z_r, \quad (3)$$

where t_f be time from the release point to the landing point. We here regard horizontal plane including point (0, 0, z_G) as the ground level. Letting $^{i}z_f = z_G$ and giving θ, ω, and $\Delta\varphi$, the landing position $^{i}\boldsymbol{P}_{\mathrm{f}}$ is obtained by eliminating t_f from (1), (2), and (3). Note that the landing position when $\Delta\varphi = 0$ is defined by $^{i}\boldsymbol{P}_{\mathrm{t}}$ ($^{i}x_t$, $^{i}y_t$, z_G). $^{i}\boldsymbol{P}_{\mathrm{t}}$ is the target position of the capsule when it is launched without any error of releasing. The landing position error based on $^{i}\boldsymbol{P}_{\mathrm{t}}$ is defined by

$$^{i}\Delta x = {}^{i}x_f - {}^{i}x_t, \quad (4)$$
$$^{i}\Delta y = {}^{i}y_f - {}^{i}y_t. \quad (5)$$

In the next place, we give specific values and examine the landing position error of the capsule to compare the two throwing methods. The parameters are given as the follows: L_b = 0.7m, g = 9.8m/s^2, θ = 45deg, and z_G = 0. In the case of underarm throw, the relation between $^{a}\Delta x$ and ω obtained by changing $\Delta\varphi$ from -10deg to 10deg is shown in Fig. 4(a). In the case of sidearm throw, the relation between $^{b}\Delta x$ and $^{b}\Delta y$ is shown in Fig. 4(b).

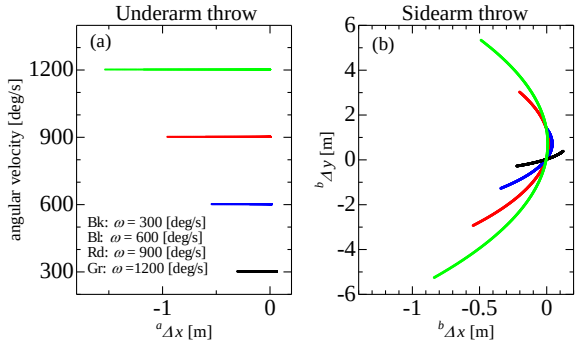

Figure 4: Landing position error by the two throws

Let us consider the error ranges of landing position, $^{i}\Delta x_{spn}$ and $^{i}\Delta y_{spn}$ in the direction of x and y axis. Letting $^{i}\Delta x_{max}$ and $^{i}\Delta x_{min}$ be the max/min of $^{i}\Delta x$, the error ranges are given by the followings: $^{i}\Delta x_{spn} = |^{i}\Delta x_{max} - {}^{i}\Delta x_{min}|$, $^{i}\Delta y_{spn} = |^{i}\Delta y_{max} - {}^{i}\Delta y_{min}|$. As shown in Fig. 4(a), the error range $^{a}\Delta x_{spn}$ increases according to ω, and its values are 0.3583, 0.5387, 0.9506, 1.5288m. On the other hand, the error range $^{b}\Delta x_{spn}$ changes as follows: 0.3450, 0.3387, 0.5445, 0.8336m. The error range $^{b}\Delta y_{spn}$ increases according to ω like $^{a}\Delta x_{spn}$, and its values are 0.6586, 2.6461, 5.9553, 10.5877m. The increase rate of $^{b}\Delta y_{spn}$ is very high as compared to that of $^{a}\Delta x_{spn}$ or $^{b}\Delta x_{spn}$. The expansion of the position error in the y direction is a disadvantage of the sidearm throw. The similar tendency is confirmed in the case when giving another value of θ and ω described above.

Consequently, the underarm throw is more available for long throw to reduce the error of landing position of the capsule. Additionally, the position error by the overarm throw is similar to that by the underarm throw.

2.3 Landing position error for release angle

We discuss how to reduce the error of landing position in the case of the underarm throw.

Figure 5 shows the error range $^{a}\Delta x_{spn}$ with respect to the release angle θ when giving z_G = –1m. Point on each curve in Fig. 5 represents the minimum error point. As shown in the figure, θ which minimizes the error range $^{a}\Delta x_{spn}$ converges to 45deg according to increase of ω. But in general, the error range increases proportional to the distance to the landing point. Therefore, the rate of the error range to the reaching distance should be evaluated.

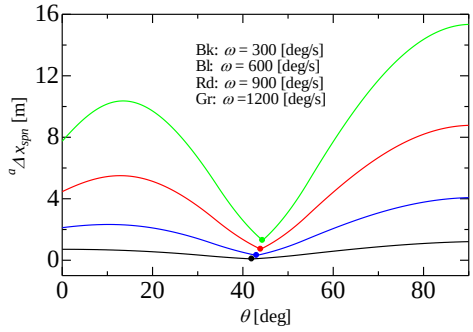

Figure 5: Landing position error with respect to release angle

Calculating $^{a}\Delta x_{spn}/|^{a}x_t|$ instead of $^{a}\Delta x_{spn}$ in the same manner as described above, the rate of the error range to the reaching distance is obtained as shown in Fig. 6. In analogy with Fig. 5, it turns out that θ which minimizes $^{a}\Delta x_{spn}/|^{a}x_t|$ converges to 45deg as ω increases.

Hence the release angle θ which reduces the error of landing position can be determined by evaluating the rate of the error range to the reaching distance.

As shown in Fig. 6, the rate of the error range is not significantly changed when ω gets doubled, from 600 deg/s to 1200deg/s. Compared to release angle error, it can be surmised that rotational speed error has little to no effect on the error of landing position.

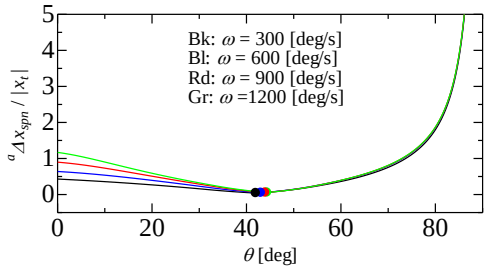

Figure 6: Landing position error with respect to release angle

3 Experiments

3.1 Experimental setup

The casting probe system is developed as shown in Fig. 7. The boom is driven by a DD motor (SGMCS-05B3C41, Yaskawa Corp.) attached at the base frame, and its angle is measured by an optical encoder (20bit). Since the hollow aluminum lumber is used for both weight saving and high rigidity of the boom, vibration during rotation of the boom is reduced. The release device equipped at the boom is driven by the solenoid. The electricity is supplied to the solenoid from outside via the slip ring. The capsule is equipped at the tip of the boom. It is gripped by four fingers of the release device. Since the fingers are supported by long swing bar, they can resist large centrifugal force thanks to leverage and be unlocked by low power to release the capsule. Diameter and width of the capsule are 120mm and 60mm. Since it is the first trial, the capsule is not real one but a dummy for early stage of experiment.

Figure 7: Experimental setup

The boom's weight, the capsule's weight, the height of the center of rotation, and the boom's length are the followings: m_0 = 11.5kg, m_1 = 1.0kg, H_0 = 1.69m, L_b = 0.7m. This system runs on a 1GHz CPU-based PC (Intel Pentium(R) III) under real time OS, ART-Linux 2.4.34. The sampling time is set at 0.001s.

3.2 Long throw

We conducted the field test of launching the capsule. The target point was set at distance 18m from the casting probe system because we can expect that it will throw the capsule more than 100m on the moon if the throw more than 16.7m is realized on earth. The desired release angle and the desired angular velocity of the boom were 44deg and 1038deg/s, respectively. Flight trajectory of the capsule is shown in Fig. 8. Red circle in the figure represents the position of the capsule. As shown in the figure, the trajectory describes a parabola and the capsule reaches the target, yellow flag.

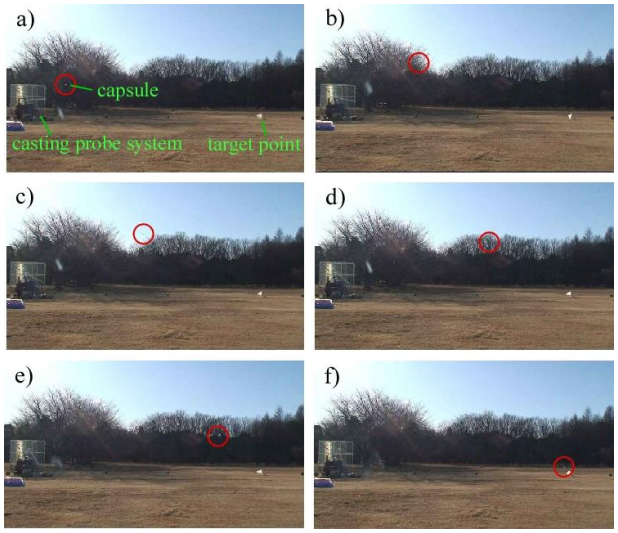

Figure 8: Flight trajectory (Field test at JAXA site)

We launched the capsule five times, and measured its landing positions by the laser range sensor. Figure 9(a) shows that distance up to the landing point with respect to trial number of launch. The standard deviation in this case is 0.1296. Since five data are distributed at the range of 0.33m between the two dotted lines, precision of landing position (repeatability) is less than 1.83% of the flight distance. Figure 9(b) shows the position error rate with respect to trial number of launch. The minimum value of the rate is 1.67% and the maximum one is 3.51%. Then, accuracy of landing position is estimated at 2.59% of the flight distance. The nearest landing point from the target is at distance 17.7m as shown in Fig. 9(a).

It means that the capsule did not reach the target distance 18m. We think the influences of air resistance and wind have greatly affected the results this time.

From these results, it can be expected that the capsule reaches on the periphery of the target with the same precision and accuracy as the test on the earth when it is launched to a distance of 100m on the moon.

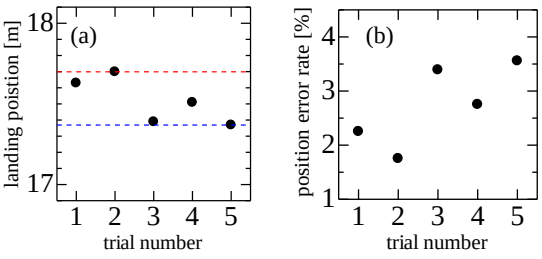

Figure 9: Landing position and its accuracy

4 Conclusions

In order to explore the underground of the moon, we proposed the method of throwing the capsule containing probe vehicle into the vertical hole in this paper. We discuss how to throw the capsule further and more precisely. The following three points are clarified:

We analyzed the error of the landing position caused by the error of the release angle in the two case of throw: the underarm throw and the side arm throw. Then it is found that the former throw is available for the error reduction.

We propose the index, i.e. the rate of the error range for the reaching distance, which enables users to select parameters of throwing to reduce the landing position error.

We verified the effectiveness of the launching control and launcher system through the experiments, and realized the throwing more than 17m and the high precision of landing position less than 1.83% of the flight distance.

Acknowledgment

This work was supported in part by the JAXA-AIST Joint Research Found.

References

[1] Haruyama, J. et al., "Possible lunar lava tube skylight observed by SELENE cameras," *Geophys. Res. Lett.*, 36, L21206, doi:10.1029/2009 GL040635, 2009.

[2] Haruyama, J., Morota, T., Kobayashi, S., Sawai, S., Lucey, P.G., Shirao, M., and Nishino, M.N., "Lunar Holes and Lava Tubes as Resources for Lunar Science and Exploration," in: *Badescu, V. (Eds.), Moon - Prospective Energy and Material Resources*, *Springer*, pp. 139-164, 2012.

[3] H. Arisumi, M. Otsuki and S. Nishida, "Launching penetrator by Casting manipulator system," *IEEE/ RSJ Int. Conf. on Intelligent Robots and Systems (IROS2012)*, Portugal, Oct. 2012.

[4] M. Kaneko, M. Higashimori, A. Namiki and M. Ishikawa, "The 100G Capturing Robot — Too Fast to See," *Robotics Research, Springer Tracts in Advanced Robotics*, Vol.15, pp.517-526, 2005.

[5] T. Tabata, and Y. Aiyama, "Tossing Manipulation by 1 degree of freedom manipulator," *IEEE/RSJ Int. Conf. on Intelligent Robots and Systems*, 2001.